The Quantum Interference Effect Transistor: Principles and Perspectives

Charles A. Stafford[1], David M. Cardamone[2], and Sumit Mazumdar[1]

[1] Department of Physics, University of Arizona, 1118 E. 4th Street, Tucson, Arizona, United States, 85721
[2] Department of Physics, Simon Fraser University, 8888 University Drive, Burnaby, British Columbia, Canada, V5A 1S6.

E-mail: stafford@physics.arizona.edu

Abstract. We give a detailed discussion of the Quantum Interference Effect Transistor (QuIET), a proposed device which exploits interference between electron paths through aromatic molecules to modulate current flow. In the off state, perfect destructive interference stemming from the molecular symmetry blocks current, while in the on state, current is allowed to flow by locally introducing either decoherence or elastic scattering. Details of a model calculation demonstrating the efficacy of the QuIET are presented, and various fabrication scenarios are proposed, including the possibility of using conducting polymers to connect the QuIET with multiple leads.

PACS numbers: 85.65.+h, 73.63.-b, 31.15.Ne, 03.65.Yz

Submitted to: *Nanotechnology (NGC2007 Special Issue)*

1. Introduction

Despite their low cost and extreme versatility, modern semiconductor transistors face fundamental obstacles to continued miniaturization. First, top-down fabrication gives them microscopic variability from device to device, which, while acceptable at today's length scales, renders them unscalable in the nanometre regime. Second, these devices, like all field effect devices, function by raising and lowering an energy barrier to charge transport of at least k_BT; each device therefore dissipates energy of this magnitude into the environment with every switching cycle. At device densities greater than the current state of the art, the cost and engineering challenges associated with removing the resultant heat are daunting [1]. While the first challenge can be met by utilizing the bottom-up, chemical fabrication of single-molecule devices, this approach in itself does nothing to address the need for a cooler switching mechanism.

An alternative paradigm to raising and lowering an energy barrier is to exploit the wave nature of the electron to control current flow [2, 3, 4, 5, 6, 7]. Traditionally, such interference-based devices are modulated via the Aharanov–Bohm effect [8]. This, however, is incompatible with the small size of molecular devices [2]: Through a nm^2 device, a magnetic field of over 600T would be required to generate a phase shift of order 1 radian. Similarly, a device based on an electrostatic phase shift [5] would require voltages incompatible with structural stability. Previously [9], we have proposed a solution, called the quantum interference effect transistor (QuIET) (see Figure 1), which exploits a perfect destructive interference due to molecular symmetry and controls quantum transport by introducing decoherence or elastic scattering.

The purpose of this article is to communicate the details of this proposal, including several potential chemical structures to facilitate fabrication and testing of this device. In Section 2, we describe the theoretical framework used to model the device. Section 3 explains the QuIET's operating mechanism. Section 4 discusses practical implementations of the device. We conclude in Section 5.

2. Theoretical Model

The QuIET consists of a central molecular element, two leads chemically bonded to the molecule, and a third lead, which can be coupled to the molecule either capacitively or via tunneling. The Hamiltonian of this system can be written as the sum of three terms:

$$H = H_{mol} + H_{leads} + H_{tun}. \tag{1}$$

The first is the π-electron molecular Hamiltonian

$$H_{mol} = \sum_{n\sigma} \varepsilon_n d^\dagger_{n\sigma} d_{n\sigma} - \sum_{nm\sigma} \left(t_{nm} d^\dagger_{n\sigma} d_{m\sigma} + \text{H.c.}\right) + \sum_{nm} \frac{U_{nm}}{2} Q_n Q_m, \tag{2}$$

where $d^\dagger_{n\sigma}$ creates an electron of spin $\sigma = \uparrow, \downarrow$ in the π-orbital of the nth carbon atom, and ε_n are the orbital energies. We use a tight-binding model for the hopping matrix elements with $t_{nm} = 2.2$eV, 2.6eV, or 2.4eV for orbitals connected by a single bond, double bond, or within an aromatic ring, respectively, and zero otherwise. The final term of Eq. (2) contains intra- and intersite Coulomb interactions, as well as the electrostatic coupling to the leads. The interaction energies are given by the Ohno

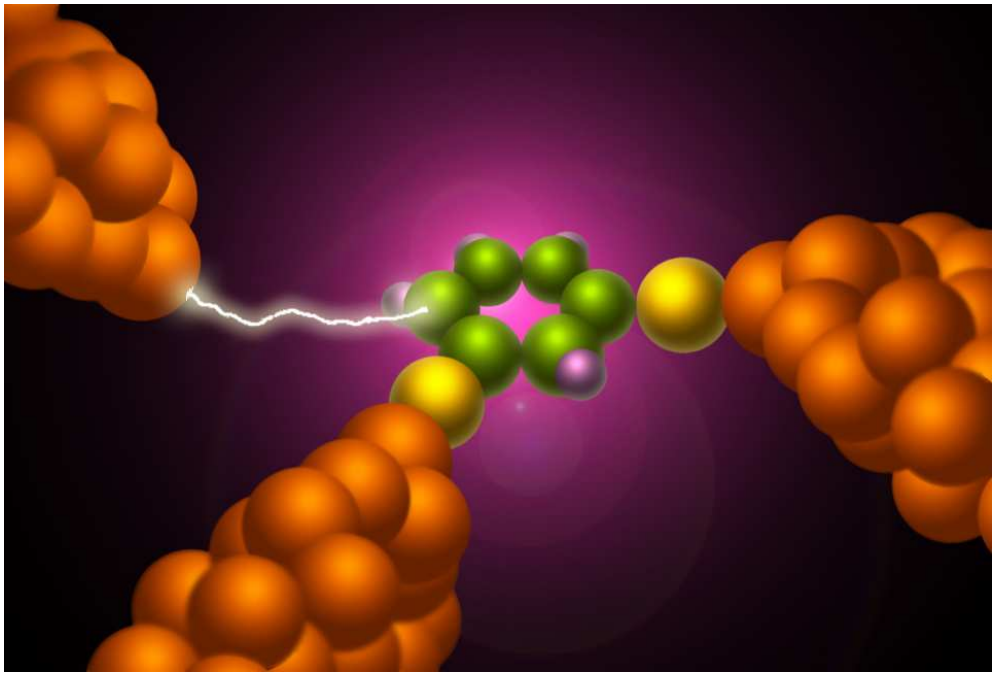

Figure 1. Artist's conception of a quantum interference effect transistor based on 1,3-benzenedithiol. The coloured spheres represent individual carbon (green), hydrogen (purple), sulfur (yellow), and gold (gold) atoms. In the "off" state of the device, destructive interference blocks the flow of current between the source (bottom) and drain (right) electrodes. Decoherence introduced by the STM tip (upper left) suppresses interference, allowing current flow. Image by Helen M. Giesel.

parameterization [13, 14]:

$$U_{nm} = \frac{11.13\text{eV}}{\sqrt{1 + .6117\left(R_{nm}/\text{Å}\right)^2}}, \tag{3}$$

where R_{nm} is the distance between orbitals n and m.

$$Q_n = \sum_\sigma d^\dagger_{n\sigma} d_{n\sigma} - \sum_\alpha C_{n\alpha}\mathcal{V}_\alpha/e - 1 \tag{4}$$

is an effective charge operator [15] for orbital n, where the second term represents a polarization charge. Here $C_{n\alpha}$ is the capacitance between orbital n and lead α, chosen consistent with the interaction energies of Eq. (3) and the geometry of the device, and $\mathcal{V}_\alpha$ is the voltage on lead α. e is the magnitude of the electron charge.

Each metal lead α possesses a continuum of states, and their total Hamiltonian is

$$H_{leads} = \sum_{\alpha=1}^{3} \sum_{\substack{k\in\alpha \\ \sigma}} \epsilon_k c^\dagger_{k\sigma} c_{k\sigma}, \tag{5}$$

where ϵ_k are the energies of the single-particle levels in the leads, and $c^\dagger_{k\sigma}$ is an electron creation operator. Here leads 1 and 2 are the source and drain, respectively, and lead 3 is the control, or gate electrode.

Tunneling between molecule and leads is provided by the final term of the Hamiltonian,

$$H_{tun} = \sum_{\langle n\alpha\rangle} \sum_{\substack{k\in\alpha \\ \sigma}} \left(V_{nk} d^\dagger_{n\sigma} c_{k\sigma} + \text{H.c.} \right), \tag{6}$$

where V_{nk} are the tunneling matrix elements from a level k within lead α to the nearby π-orbital n of the molecule. Coupling of the leads to the molecule via molecular chains, as may be desirable for fabrication purposes, can be included in the effective V_{nk}, as can the effect of substituents (e.g., thiol groups) used to bond the leads to the molecule [16, 17].

We use the non-equilibrium Green function (NEGF) approach [18, 19] to describe transport in this open quantum system. The retarded Green function of the full system is

$$G(E) = \left[E - H_{mol} - \Sigma(E) \right]^{-1}, \tag{7}$$

where Σ is an operator, known as the retarded self-energy, describing the coupling of the molecule to the leads. The QuIET is intended for use at room temperature, and operates in a voltage regime where there are no unpaired electrons in the molecule. Thus lead-lead and lead-molecule correlations, such as the Kondo effect, do not play an important role. Electron-electron interactions may therefore be included via the self-consistent Hartree-Fock method. H_{mol} is replaced by the corresponding mean-field Hartree-Fock Hamiltonian H^{HF}_{mol}, which is quadratic in electron creation and annihilation operators, and contains long-range hopping. Within mean-field theory, the self-energy is a diagonal matrix

$$\Sigma_{n\sigma,m\sigma'}(E) = \delta_{nm}\delta_{\sigma\sigma'} \sum_{\langle a\alpha\rangle} \delta_{na} \Sigma_\alpha(E), \tag{8}$$

with nonzero entries on the π-orbitals adjacent to each lead α:

$$\Sigma_\alpha(E) = \sum_{\substack{k\in\alpha \\ \langle n\alpha\rangle}} \frac{|V_{nk}|^2}{E - \epsilon_k + i0^+}. \tag{9}$$

The imaginary parts of the self-energy matrix elements determine the Fermi's Golden Rule tunneling widths

$$\Gamma_\alpha(E) \equiv -2\,\mathrm{Im}\Sigma_\alpha(E) = 2\pi \sum_{k\in\alpha} |V_{nk}|^2 \delta\left(E - \epsilon_k\right). \tag{10}$$

As a consequence, the molecular density of states changes from a discrete spectrum of delta functions to a continuous, width-broadened distribution. We take the broad-band limit [18], treating Γ_α as constants characterizing the coupling of the leads to the molecule. Typical estimates [17] using the method of Ref. [20] yield $\Gamma_\alpha \lesssim 0.5$eV, but values as large as 1eV have been suggested [16].

The effective hopping and orbital energies in H^{HF}_{mol} depend on the equal-time correlation functions, which are found in the NEGF approach to be

$$\langle d^\dagger_{n\sigma} d_{m\sigma} \rangle = \sum_{\langle a\alpha\rangle} \frac{\Gamma_\alpha}{2\pi} \int_{-\infty}^{\infty} dE\, G_{n\sigma,a\sigma}(E) G^*_{a\sigma,m\sigma}(E) f_\alpha(E), \tag{11}$$

where $f_\alpha(E) = \{1 + \exp[(E-\mu_\alpha)/k_BT]\}^{-1}$ is the Fermi function for lead α. Finally, the Green function is determined by iterating the self-consistent loop, Eqs. (7)–(11).

The current in lead α is given by the multi-terminal current formula [21]

$$I_\alpha = \frac{2e}{h} \sum_{\beta=1}^{3} \int_{-\infty}^{\infty} dE\, T_{\beta\alpha}(E) \left[f_\beta(E) - f_\alpha(E) \right], \tag{12}$$

where

$$T_{\beta\alpha}(E) = \Gamma_\beta \Gamma_\alpha |G_{ba}(E)|^2 \tag{13}$$

is the transmission probability [19] from lead α to lead β, and $a\,(b)$ is the orbital coupled to lead $\alpha\,(\beta)$. Similar mean-field NEGF calculations have been widely used to treat two-terminal transport through single molecules [11].

3. Switching Mechanism

The QuIET exploits quantum interference stemming from the symmetry of monocyclic aromatic annulenes such as benzene. Quantum transport through single benzene molecules with two metallic leads connected at *para* positions has been the subject of extensive experimental and theoretical investigation [11]; however, a QuIET based on benzene requires the source (1) and drain (2) to be connected at *meta* positions, as illustrated in Fig. 1. The transmission probability T_{12} of this device, for $\Sigma_3 = 0$, is shown in Fig. 2. Due to the molecular symmetry [6], there is a node in $T_{12}(E)$, located midway between the HOMO and LUMO energy levels (see Figure 2b, lowest curve). This mid-gap node, at the Fermi level of the molecule, plays an essential role in the operation of the QuIET.

The existence of a transmission node for the meta connection can be understood in terms of the Feynman path integral formulation of quantum mechanics [22], according to which an electron moving from lead 1 to lead 2 takes all possible paths within the molecule; observables relate only to the complex sum over paths. In the absence of a third lead ($\Sigma_3 = 0$), these paths all lie within the benzene ring. An electron entering the molecule at the Fermi level has de Broglie wavevector $k_F = \pi/2d$, where $d = 1.397$Å is the intersite spacing of benzene (note that k_F is a purely geometrical quantity, which is unaltered by electron-electron interactions [23]). The two most direct paths through the ring have lengths $2d$ and $4d$, with a phase difference $k_F 2d = \pi$, so they interfere destructively. Similarly, all of the paths through the ring cancel exactly in a pairwise fashion, leading to a node in the transmission probability at $E = \varepsilon_F$.

This transmission node can be lifted by introducing decoherence or elastic scattering that break the molecular symmetry. Figures 2b and c illustrate the effect of coupling a third lead to the molecule, introducing a complex self-energy $\Sigma_3(E)$ on the π-orbital adjacent to that connected to lead 1 or 2. An imaginary self-energy $\Sigma_3 = -i\Gamma_3/2$ corresponds to coupling a third metallic lead directly to the benzene molecule, as shown in Fig. 1. If the third lead functions as an infinite-impedance voltage probe, the effective two-terminal transmission is [10]

$$\tilde{T}_{12} = T_{12} + \frac{T_{13} T_{32}}{T_{13} + T_{32}}. \tag{14}$$

The third lead introduces decoherence [10] and additional paths that are not canceled, thus allowing current to flow, as shown in Fig. 2b. As a proof of principle, a QuIET could be constructed using a scanning tunneling microscope tip as the third lead (cf. Figure 1), with tunneling coupling $\Gamma_3(x)$ to the appropriate π-orbital of the

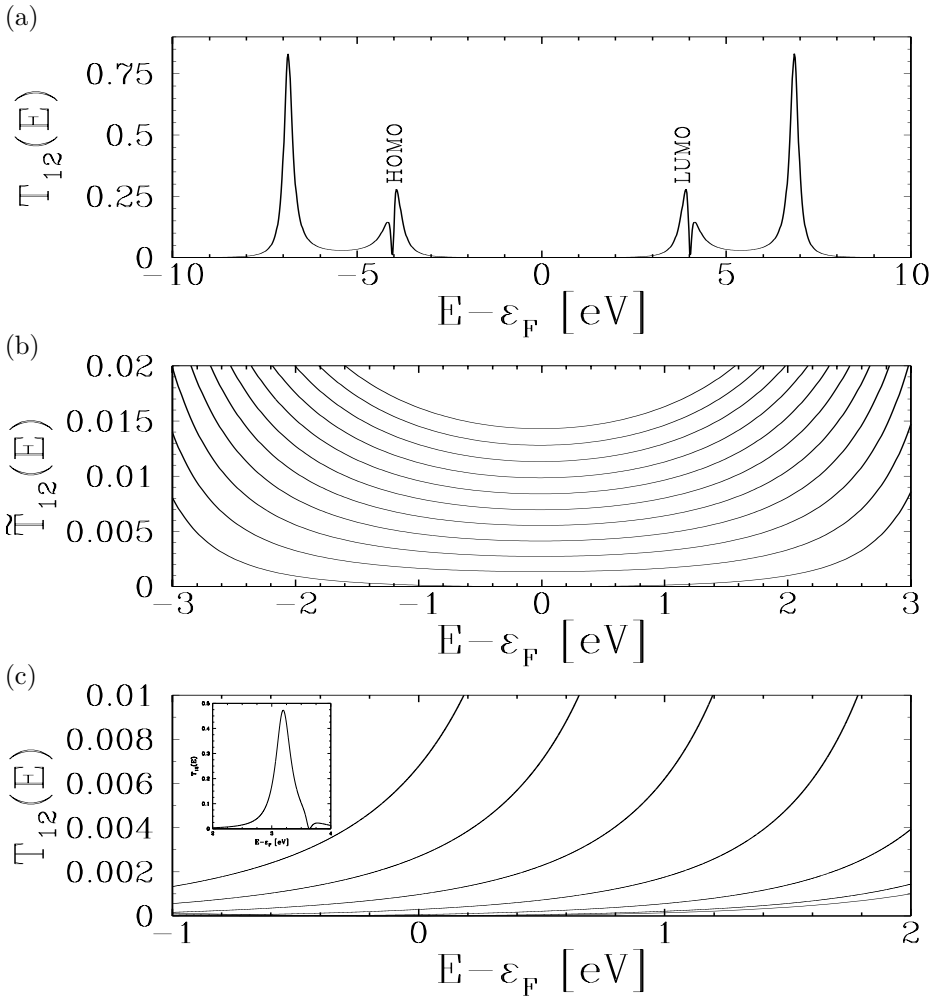

Figure 2. Effective transmission probability $\tilde{T}_{12}$ of the device shown in Fig. 1, at room temperature, with $\Gamma_1 = 1.2$eV and $\Gamma_2 = .48$eV. Here ε_F is the Fermi level of the molecule. (a) $\Sigma_3 = 0$; (b) $\Sigma_3 = -i\Gamma_3/2$, where $\Gamma_3 = 0$ in the lowest curve, and increases by .24eV in each successive one; (c) Σ_3 is given by Eq. (15) with a single resonance at $\varepsilon_\nu = \varepsilon_F + 4$eV. Here $t_\nu = 0$ in the lowest curve, and increases by 0.5eV in each successive curve. Inset: Full vertical scale for $t_\nu = 1$eV. From Ref. [9].

benzene ring, the control variable x being the piezo-voltage controlling the tip-molecule distance.

By contrast, a real self-energy Σ_3 introduces elastic scattering, which can also break the molecular symmetry. This can be achieved by attaching a second molecule to the benzene ring, for example an alkene chain. The retarded self-energy due to the presence of a second molecule is

$$\Sigma_3(E) = \sum_\nu \frac{|t_\nu|^2}{E - \varepsilon_\nu + i0^+}, \tag{15}$$

where ε_ν is the energy of the νth molecular orbital of the second molecule, and t_ν

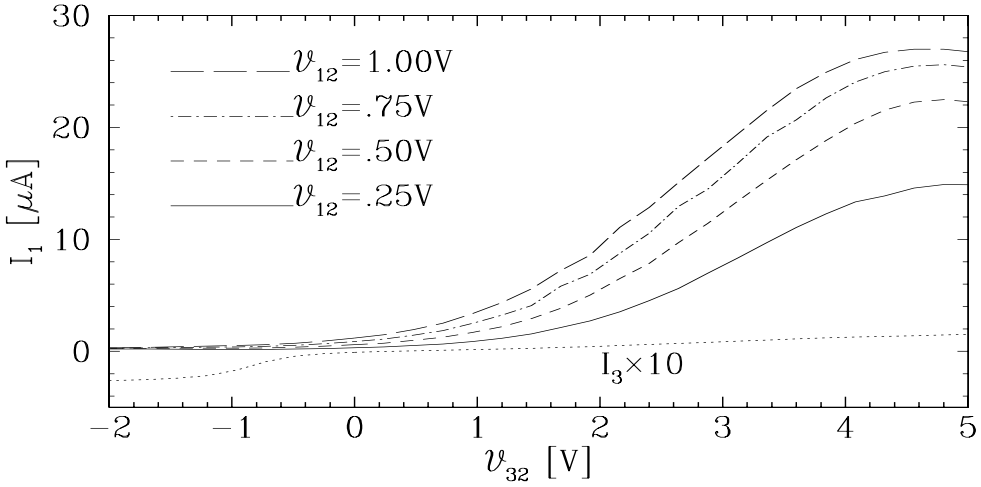

Figure 3. Room temperature I–$\mathcal{V}$ characteristic of a QuIET based on sulfonated vinylbenzene. The current in lead 1 is shown, where $\mathcal{V}_{\alpha\beta} = \mathcal{V}_\alpha - \mathcal{V}_\beta$. Here, $\Gamma_1 = \Gamma_2$ =1eV. Γ_3 is taken as .0024eV, which allows a small current in the third lead, so that the device amplifies current. A field-effect device with almost identical I–$\mathcal{V}$ can be achieved by taking $\Gamma_3 = 0$. The curve for I_3 is for the case of 1.00V bias voltage; I_3 for other biases look similar. From Ref. [9].

is the hopping integral coupling this orbital with the neighboring π-orbital of the benzene ring. Figure 2c shows the transmission probability $T_{12}(E)$ in the vicinity of the Fermi energy of the molecule, for the case of a single side-orbital at $\varepsilon_\nu = \varepsilon_F + 4$eV. As the coupling t_ν is increased, the node in transmission at $E = \varepsilon_F$ is lifted due to scattering from the side orbital. The sidegroup introduces Fano antiresonances [3, 24], which suppress current through one arm of the annulene, thus lifting the destructive interference. Put another way, the second molecule's orbitals hybridize with those of the annulene, and a state that connects leads 1 and 2 is created in the gap [see Figure 2c (inset)]. In practice, either t_ν or ε_ν might be varied to control the strength of Fano scattering.

Tunable current suppression occurs over a broad energy range, as shown in Fig. 2b; the QuIET functions with any metallic leads whose work function lies within the annulene gap. Fortunately, this is the case for many bulk metals, among them palladium, iridium, platinum, and gold [25]. Appropriately doped semiconductor electrodes [12] could also be used.

We show in Fig. 3 the I–$\mathcal{V}$ characteristic of a QuIET based on sulfonated vinylbenzene. The three metallic electrodes were taken as bulk gold, with $\Gamma_1 = \Gamma_2 = 1$eV, while $\Gamma_3 = .0024$eV, so that the coupling of the third electrode to the alkene sidegroup is primarily electrostatic. The device characteristic resembles that of a macroscopic transistor. As the voltage on lead 3 is increased, scattering from the antibonding orbital of the alkene sidegroup increases as it approaches the Fermi energies of leads 1 and 2, leading to a broad peak in the current. For $\Gamma_{1,2} \gg \Gamma_3 \neq 0$, the device amplifies the current in the third lead (dotted curve), emulating a bipolar junction transistor. Alkene chains containing 4 and 6 carbon atoms were also studied, yielding devices with characteristics similar to that shown in Fig. 3, with the maximum current I_1 shifting to smaller values of $\mathcal{V}_{32}$ with increasing chain length. As evidence

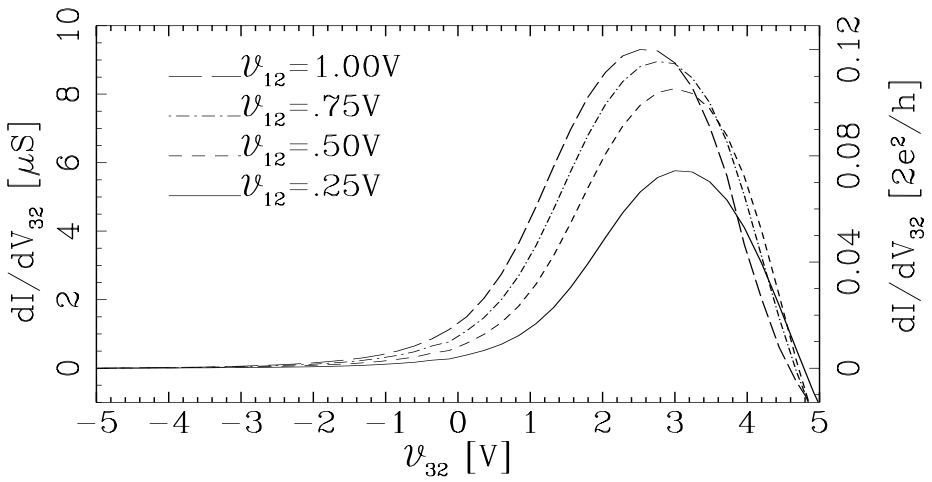

Figure 4. Transconductance $dI/d\mathcal{V}_{32}$ of a QuIET based on sulfonated vinylbenzene with $\Gamma_3 = 0$. The characteristic is similar to that of a field-effect transistor, *i.e.* $I_3 = 0$ while $I_1 = -I_2 = I$. As in Fig. 3, $\Gamma_1 = \Gamma_2 = 1$eV, and the calculation was done for room temperature. From Ref. [9].

that the transistor behavior shown in Fig. 3 is due to the tunable interference mechanism discussed above, we point out that if hopping between the benzene ring and the alkene sidegroup is set to zero, so that the coupling of the sidegroup to benzene is purely electrostatic, almost no current flows between leads 1 and 2.

For $\Gamma_3 = 0$, $I_3 = 0$ and the QuIET behaves as a field-effect transistor. The transconductance $dI/d\mathcal{V}_{32}$ of such a device is shown in Fig. 4. For comparison, we note that an ideal single-electron transistor [26] with $\Gamma_1 = \Gamma_2 = 1e$V has peak transconductance $(1/17)G_0$ at bias voltage .25V, and $(1/2)G_0$ at bias 1V, where $G_0 = 2e^2/h$ is the conductance quantum. For low biases, the proposed QuIET thus has a higher transconductance than the prototypical nanoscale amplifier, while even for large biases its peak transconductance is comparable. Likewise, the load resistances required for a QuIET to have gain (load times transconductance) greater than one while in its "on" state are comparable to other nanoscale devices, $\sim 10/G_0$.

Operation of the QuIET does not depend sensitively on the magnitude of the lead-molecule coupling $\bar{\Gamma} = \Gamma_1\Gamma_2/(\Gamma_1+\Gamma_2)$. The current through the device decreases with decreasing $\bar{\Gamma}$, but aside from that, the device characteristic was found to be qualitatively similar when $\bar{\Gamma}$ was varied over one order of magnitude. The QuIET is also insensitive to molecular vibrations: only vibrational modes that simultaneously alter the carbon-carbon bond lengths and break the six-fold symmetry within the benzene component can cause decoherence in a benzene 'interferometer.' Such modes are only excited at temperatures greater than about 500K.

The position of the third lead affects the degree to which destructive interference is suppressed. For benzene, the most effective location for the third lead is shown in Fig. 1. It may also be placed at the site immediately between leads 1 and 2, but the transistor effect is somewhat reduced, since coupling to the charge carriers is less. The third, three-fold symmetric configuration of leads completely decouples the third lead from electrons traveling between the first two leads. For each monocyclic aromatic

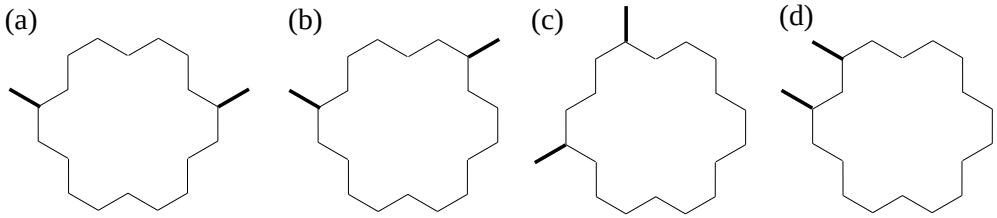

Figure 5. Source-drain lead configurations possible in a QuIET based on [18]-annulene. The bold lines represent the positioning of the two leads. Each of the four arrangements has a different phase difference associated with it: (a) π; (b) 3π; (c) 5π; and (d) 7π. From Ref. [9].

annulene, one three-fold symmetric lead configuration exists, yielding no transistor behavior.

The QuIET's operating mechanism, tunable coherent current suppression, occurs over a broad energy range within the gap of each monocyclic aromatic annulene; it is thus a *very robust effect, insensitive to moderate fluctuations of the electrical environment of the molecule.* Although based on an entirely different, quantum mechanical, switching mechanism, the QuIET nonetheless reproduces the functionality of macroscopic transistors on the scale of a single molecule.

4. Implementations

As daunting as the fundamental problem of the switching mechanism is the practical one of nanofabrication. The QuIET requires a third lead coupled locally to the central molecule, and, while there has recently been significant progress in that direction [12, 27, 28], to date, only two-lead single molecular devices, sometimes with global gating, have been achieved [11]. With this in mind, we turn to potential practical realizations of the device.

Using novel fabrication techniques, such as ultra-sharp STM tips [27] or substrate pitting [28], it may soon be possible to attach multiple leads to large molecules. Fortunately, the QuIET mechanism applies not only to benzene, but to any monocyclic aromatic annulene with leads 1 and 2 positioned so the two most direct paths have a phase difference of π. Furthermore, larger molecules have other possible lead configurations, based on phase differences of 3π, 5π, etc.; as an example, Figure 5 shows the lead configurations for a QuIET based on [18]annulene. Other large ring-like molecules, such as [14]annulene and divalent metal-phthalocyanine, would also serve well.

Another method of increasing the effective size of the molecule is to introduce molecular wires linking the central ring and leads (see Figures 6 and 7). Conducting polymers, such as polythiophene or polyaniline, are ideal for this task. Such changes can be absorbed into the diagonal elements of the self-energy $\Sigma(E)$, and so only modify $G(E)$ locally. As such, while they can significantly modify the on-resonance behavior of a molecular device, off-resonance function is largely unaltered. In particular, the transmission node at the centre of the gap is unaffected. An example of such a QuIET integrated with conventional circuitry on a chip is shown in Figure 7.

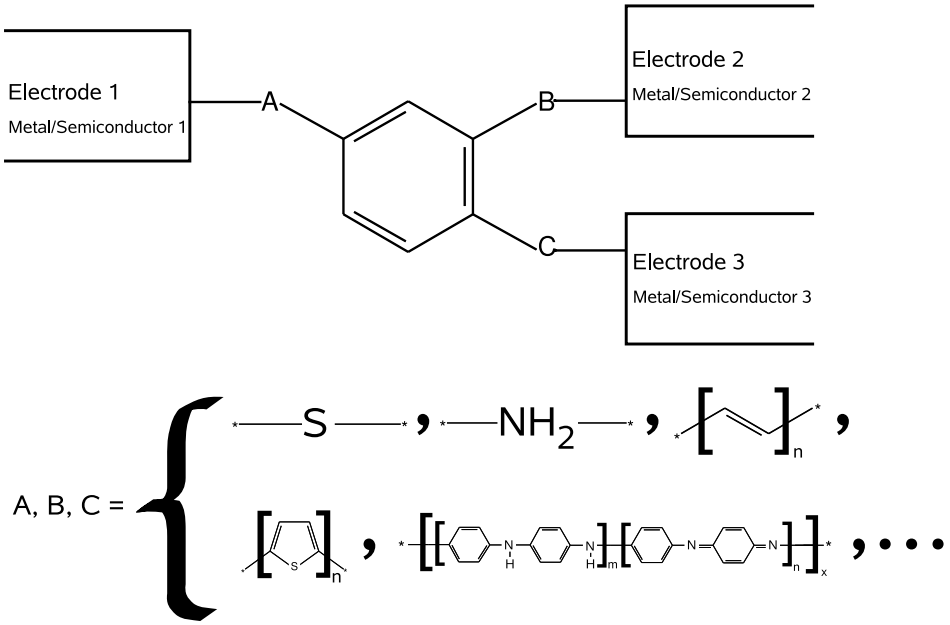

Figure 6. Schematic of various QuIETs based on a benzene ring. A, B, and C represent the various substituents which may be placed in series between the ring and each lead. In particular, the conducting polymers like polyaniline and polythiophene may be useful in overcoming the "third lead" problem.

5. Conclusions

The quantum interference effect transistor represents one way to simultaneously overcome the problems of scalability and power dissipation which face the next generation of transistors. Because of the exact symmetry possible in molecular devices, it possesses a perfect mid-gap transmission node, which serves as the off state for the device. Tunably introduced decoherence or elastic scattering can lift this quantum interference effect, with the result of current modulation. Furthermore, a vast variety of potential chemical structures possess the requisite symmetry, easing fabrication difficulties. In particular, molecular wires, such as conducting polymers, can be used to extend the molecule to arbitrary size.

Acknowledgments

This work was supported in part by National Science Foundation Grant Nos. PHY0210750, DMR0312028, and DMR0406604.

References

[1] *International Technology Roadmap for Semiconductors: 2006 Update,* `http://public.itrs.net`.
[2] Sautet, P.; Joachim, C. *Chem. Phys. Lett.* **1988,** *153,* 511.
[3] Sols, F.; Macucci, M.; Ravaioli, U.; Hess, K. *Appl. Phys. Lett.* **1989,** *54,* 350.

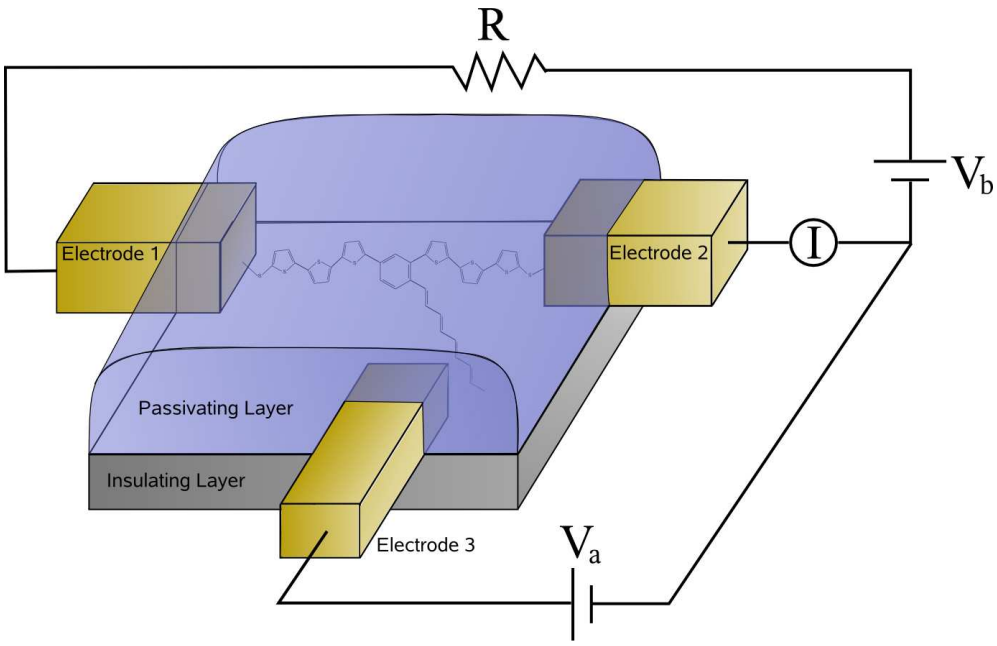

Figure 7. Possible embodiment of a QuIET integrated with conventional circuitry on a chip. The source (1) and drain (2) electrodes are connected via conducting polymers (in this case, polythiophene) to the central aromatic ring, while the gate electrode (3) is coupled electrostatically to an alkene sidegroup.

[4] Joachim, C.; Gimzewski, J. K. *Chem. Phys. Lett.* **1997,** *265,* 353. Joachim, C.; Gimzewski, J. K.; Tang, H. *Phys. Rev. B* **1998,** *58,* 16407.
[5] Baer, R.; Neuhauser, D. *J. Am. Chem. Soc.* **2002,** *124,* 4200.
[6] Yaliraki, S. N.; Ratner, M. A. *Ann. N.Y. Acad. Sci.* **2002,** *960,* 153.
[7] Stadler, R.; Forshaw, M.; Joachim, C. *Nanotechnology* **2003,** *14,* 138. Stadler, R.; Ami, S.; Forshaw, M.; Joachim, C. *Nanotechnology* **2003,** *14,* 722.
[8] Washburn, S.; Webb, R. A. *Adv. Phys.* **1986,** *35,* 375.
[9] Cardamone DM, Stafford CA, and Mazumdar S 2006 *Nano Lett.* **6** 2422
[10] Büttiker, M. *IBM J. Res. Dev.* **1988,** *32,* 63.
[11] Nitzan, A.; Ratner, M. A. *Science (Washington, D.C.)* **2003,** *300,* 1384, and references therein.
[12] Piva, P. G.; DiLabio, G. A.; Pitters, J. L.; Zikovsky, J.; Rezeq, M.; Dogel, S.; Hofer, W. A.; Wolkow, R. A. *Nature (London)* **2005,** *435,* 658.
[13] Ohno, K. *Theor. Chim. Acta* **1964,** *2,* 219.
[14] Chandross, M.; Mazumdar, S.; Liess, M.; Lane, P. A.; Vardeny, Z. V.; Hamaguchi, M.; Yoshino, K. *Phys. Rev. B* **1997,** *55,* 1486.
[15] Stafford, C. A.; Kotlyar, R.; Das Sarma, S. *Phys. Rev. B* **1998,** *58,* 7091.
[16] Tian, W.; Datta, S.; Hong, S.; Reifenberger, R.; Henderson, J. I.; Kubiak, C. P. *J. Chem. Phys.* **1998,** *109,* 2874.
[17] Nitzan, A. *Annu. Rev. Phys. Chem.* **2001,** *52,* 681.
[18] Jauho, A.-P.; Wingreen, N. S.; Meir, Y. *Phys. Rev. B* **1994,** *50,* 5528.
[19] Datta, S. *Electronic Transport in Mesoscopic Systems;* Cambridge University Press, Cambridge, UK, 1995, pp 293-342.
[20] Mujica, V.; Kemp, M.; Ratner, M. A. *J. Chem. Phys.* **1994,** *101,* 6849.
[21] Büttiker, M. *Phys. Rev. Lett.* **1986,** *57,* 1761.
[22] Feynman, R. P.; Hibbs, A. R. *Quantum Mechanics and Path Integrals;* McGraw-Hill, New York, 1965.
[23] Luttinger, J. M.; *Phys. Rev.* **1960,** *119,* 1153.
[24] Clerk, A. A.; Waintal, X.; Brouwer, P. W. *Phys. Rev. Lett.* **2001,** *86,* 4636.
[25] Marder, M. P. *Condensed Matter Physics;* John Wiley & Sons, Inc., New York, 2000.

[26] Kastner, M. A. *Rev. Mod. Phys.* **1992,** *64,* 849.
[27] Rezeq M, Pitters J, and Wolkow R 2006 *J. Chem. Phys.* **124** 204716
[28] Mativetsky JM, Burke SA, Fostner S, and Grutter P 2007 Nanoscale pits as templates for building a molecular device *Small 3,* 818.